Journal of Neurochemistry

JOURNAL OF NEUROCHEMISTRY | 2014

doi: 10.1111/jnc.12733

ORIGINAL ARTICLE

Voltammetric and mathematical evidence for dual transport mediation of serotonin clearance *in vivo*

Kevin M. Wood,* Anisa Zeqja,* H. Frederik Nijhout,† Michael C. Reed,‡ Janet Best§ and Parastoo Hashemi*

*Department of Chemistry, Wayne State University, Detroit, Michigan, USA

†Department of Biology, Duke University, Durham, North Carolina, USA

‡Department of Mathematics, Duke University, Durham, North Carolina, USA

§Department of Mathematics, The Ohio State University, Columbus, Ohio, USA

Abstract

The neurotransmitter serotonin underlies many of the brain's functions. Understanding serotonin neurochemistry is important for improving treatments for neuropsychiatric disorders such as depression. Antidepressants commonly target serotonin clearance via serotonin transporters and have variable clinical effects. Adjunctive therapies, targeting other systems including serotonin autoreceptors, also vary clinically and carry adverse consequences. Fast scan cyclic voltammetry is particularly well suited for studying antidepressant effects on serotonin clearance and autoreceptors by providing real-time chemical information on serotonin kinetics *in vivo*. However, the complex nature of *in vivo* serotonin responses makes it difficult to interpret experimental data with established kinetic models. Here, we electrically stimulated the mouse medial forebrain bundle to provoke and detect terminal serotonin in the substantia nigra reticulata. In response to medial forebrain bundle stimulation we found three dynamically distinct serotonin signals. To interpret these signals we developed a computational model that supports two independent serotonin reuptake mechanisms (high affinity, low efficiency reuptake mechanism, and low affinity, high efficiency reuptake system) and bolsters an important inhibitory role for the serotonin autoreceptors. Our data and analysis, afforded by the powerful combination of voltammetric and theoretical methods, gives new understanding of the chemical heterogeneity of serotonin dynamics in the brain. This diverse serotonergic matrix likely contributes to clinical variability of antidepressants.

Keywords: 5-HT, computational neuroscience, methiothepin, Michaelis–Menten, SERT, transport.

J. Neurochem. (2014) 10.1111/jnc.12733

Serotonin is an important neurotransmitter because of its involvement in depression, which lowers mood and self-esteem and is among the most prevalent health problems in the USA (Gonzalez *et al.* 2010). The most popular antidepressants are the selective serotonin reuptake inhibitors (SSRIs). SSRIs inhibit serotonin transporters (SERTs), which extend the lifetime of serotonin in the synapse. These agents can take weeks to reach clinical effectiveness (Gelenberg and Chesen 2000), have variable benefits, and carry harsh side effects (Ferguson 2001; Masand and Gupta 2002; Cipriani *et al.* 2009). Moreover, many patients fail to experience full remission after antidepressant therapy (Souery *et al.* 2006); thus, supplemental therapies targeting the serotonin autoreceptors, in addition to dopaminergic and noradrenergic receptors, are often coprescribed with SSRIs (Richelson and Souder 2000; Davies *et al.* 2004; Alexander *et al.* 2011). The clinical effectiveness of these adjunctive strategies, such as the atypical anti-psychotics Abilify™ and Seroquel™, remains variable (Spielmans *et al.* 2013) and their mode of action is not well understood in depression (Yatham *et al.* 2005). It is likely that their impact on the serotonin autoreceptors is important because a wealth of literature implicates the autoreceptors in antidepressant mechanisms (Chaput *et al.* 1986; Blier *et al.* 1987; Le Poul *et al.* 1995; Riad *et al.* 2004). Therefore, the neurochemistry that under-

Received February 2, 2014; revised manuscript received March 25, 2014; accepted April 2, 2014.

Address correspondence and reprint requests to Parastoo Hashemi, Department of Chemistry, Wayne State University, 5101 Cass Avenue, Detroit, MI 48202, USA. E-mail: phashemi@chem.wayne.edu

Abbreviations used: DRN, dorsal raphe nucleus; FIA, flow injection analysis; FSCV, fast scan cyclic voltammetry; MFB, medial forebrain bundle; NET, norepinephrine transporter; OCT, organic cation transporter; SERTs, serotonin transporters; SSRIs, selective serotonin reuptake inhibitors.

lies serotonin release and transport is a critical field of study to better understand antidepressant mechanisms.

Fast scan cyclic voltammetry (FSCV) is a powerful tool for studying real-time neurochemistry in a living mammalian nervous system. FSCV has uncovered differences between serotonin and dopamine regulation *in vivo* (Hashemi *et al.* 2012). Briefly, serotonin is highly regulated, difficult to evoke electrically, and is mechanistically more driven by reuptake and metabolism than synthesis and vesicular packaging (Hashemi *et al.* 2012). Acute SSRI administration in mice rapidly decreases serotonin clearance. This process is not static but changes dynamically over 2 h (Wood and Hashemi 2013). In contrast, acute serotonin autoreceptor antagonism had modest effects on serotonin release amplitude and clearance (Hashemi *et al.* 2012). From these studies, it is clear that the chemical cascades following SSRI and autoreceptor treatments are complicated. Understanding this chemistry is the key to designing better pharmacological agents. The first step toward this goal is to investigate endogenous serotonin clearance and autoreceptor control.

In this work, we utilized FSCV to measure serotonin in the mouse substantia nigra pars reticulata (SNr) upon medial forebrain bundle (MFB) stimulation. We discovered a phenomenon that may better direct antidepressant studies. We found three distinct serotonin responses to the same electrical stimulation. We term these responses fast, slow, and hybrid based on differences in clearance curves.

By extending prior models that study serotonin kinetics in tissue slice preparations (Bunin and Wightman 1998; Bunin *et al.* 1998), we developed a Michaelis–Menten kinetic model to interpret our *in vivo* data. Our mathematical model showed that the three distinct responses can be understood as different combinations of two clearance or 'reuptake' mechanisms, one with high affinity and low efficiency and one with low affinity and high efficiency. Indeed, in 1970, Snyder and coworkers proposed two distinct reuptake mechanisms for serotonin, which they termed 'Uptake 1' and 'Uptake 2' (Shaskan and Snyder 1970). More recently, Daws and coworkers pharmacologically distinguished between the transporters responsible for Uptake 1 and Uptake 2 and outlined the importance of targeting non-SERT transporters in antidepressant therapies (Daws *et al.* 2013; Horton *et al.* 2013). The kinetics of our two reuptake mechanisms agree well with Uptake 1 and Uptake 2. We found that administration of Escitalopram, a popular SSRI, not only largely inhibited Uptake 1 mechanisms but also, to a lesser extent, inhibited Uptake 2 mechanisms. Our model additionally showed that a strong autoreceptor effect is necessary to explain a descent of extracellular serotonin below baseline after stimulation. Autoreceptor modulation was confirmed experimentally by treating mice with methiothepin, an autoreceptor antagonist, which abolished serotonin's descent below baseline. This finding is the first rapid chemically resolved evidence of autoreceptor function.

Our voltammetric experiments and computational analyses present three dynamic serotonin clearance patterns, support two distinct reuptake mechanisms for serotonin, and suggest that serotonin is under a rapid, sophisticated level of autoreceptor control. Combined, our novel approach is a powerful platform from which to study the highly complex serotonergic release and reuptake machinery.

Materials and methods

Animals

Male C57BL/6J mice (Jackson Laboratory, Bar Harbor, ME, USA) weighing 20–25 g were used in stereotaxic surgeries (David Kopf Instruments, Tujunga, CA, USA). Animal procedures were in agreement with *The Guide for the Care and Use of Laboratory Animals,* accepted by the Institutional Animal Care and Use Committees (IACUC) of Wayne State University. Mice were housed in 12-h light/dark cycles and were presented food and water *ad libitum*.

Surgical procedures

Before surgery, mice were injected into the intraperitoneal space with 25% urethane dissolved in 0.9% sodium chloride (Hospira, Lake Forest, IL, USA) at a volume of 7 μL per 1 g mouse weight. Ideal mouse body temperature (37°C) was maintained using a heating pad (Braintree Scientific, Braintree, MA, USA). Surgeries were performed on a stereotaxic frame (David Kopf Instruments, CA, USA). A stainless steel stimulating electrode (diameter: 0.2 mm; Plastics One, Roanoke, VA, USA) was implanted into the MFB and a microelectrode coated with Nafion (Hashemi *et al.* 2009) was lowered into the SNr as in previous studies (Wood and Hashemi 2013). Bregma was used as reference for stereotaxic coordinates of MFB [AP: −1.58, ML: +1.10, DV: −4.8–5.0] and SNR [AP: −3.28, ML: +1.40, DV: −4.2] from Paxinos and Franklin (2008). Holes were drilled to access the SNr and MFB. Hydrochloric acid (0.1 M, 4 V vs. tungsten) was used to electroplate chloride onto a silver wire (diameter: 0.010 in; A-M Systems, Sequim, WA, USA). The resulting Ag/AgCl reference electrode was positioned in the opposite hemisphere of the hole drilled for the SNr electrode placement. A 60 Hz biphasic 350 μA, 120 pulse stimulation, 2 ms per phase were employed through a linear constant current stimulus isolator (NL800A Neurolog; Digitimer Ltd, Hertfordshire, UK). Methiothepin mesylate (20 mg kg^{-1}) and Escitalopram oxalate (100 mg kg^{-1}) were dissolved in saline and injected into the intraperitoneal cavity and obtained from Sigma-Aldrich (St. Louis, MO, USA).

Electrochemical procedures

The carbon fiber microelectrodes were prepared by aspiration of carbon fibers (T- 650; diameter: 7 μm; Goodfellow, Coraopolis, PA, USA) into glass capillaries (external diameter: 0.6 mm, internal diameter: 0.4 mm; A-M Systems). The filled glass capillaries were then pulled under gravity in a micropipette puller (Narishige Group, Setagaya-Ku, Tokyo, Japan). The carbon fibers distended from the glass capillaries were cut to approximately 150 μm and were subsequently coated with Nafion. Electrodeposition of Nafion was formerly described (Hashemi *et al.* 2009). Data acquisition and

waveform application were performed via a PCIe-6341 DAC/ADC card (National Instruments, Austin, TX, USA). Custom hardware and software (WCCV 2.0) written by Christopher W. Atcherley and Michael L. Heien using LabVIEW 2012 (National Instruments) was used for voltammetry. A CHEM-CLAMP potentiostat (Dagan Corporation, Minneapolis, MN, USA) was used to measure current. For serotonin detection the carbon fiber microelectrode was scanned at 1000 V s^{-1} at 10 Hz from −0.1 V to 1.0 V, while holding at 0.2 V (Jackson *et al.* 1995). The calibration factor of serotonin for these electrodes and with the aforementioned waveform was taken from Hashemi *et al.* (2009).

Flow injection analysis

A short 1/8 nut (PEEK P-335; IDEX, Middleboro, MA, USA) was used to secure a nafion-electrocoated carbon-fiber microelectrode. The electrode/nut assembly was screwed onto a modified HPLC elbow joint (Elbow, PEEK 3432, IDEX) connected to the output of the flow injection analysis (FIA) system. The FIA system is a six-port HPLC injector with a two-position actuator (Rheodyne model 7010 valve and 5701 actuator). Tris buffer [for constituents see (Hashemi *et al.* 2011b)] was used as the flow injection buffer at a flow rate of 2 mL min^{-1} via a syringe infusion pump (kd Scientific, model KDS-410, Holliston, MA, USA). Serotonin hydrochloride (Sigma-Aldrich, St. Louis, MO, USA) was injected at fixed volume into the flow stream and reached the electrode as a square injection.

Data modeling

The simulations were carried out in MatLab R2011a (MathWorks, Natick, MA, USA) using ODE solver ode23s, implemented on an iMAC with operating system OS X Version 10.6.8.

Data analysis

Custom software was written for data analysis in Labview. 2012 by Christopher Atcherley and Michael Heien (University of Arizona). The data were firstly background subtracted to remove a large capacitative current, a consequence of the high scan rates employed. The data were then filtered at zero phase using a fourth-order Butterworth with a low pass of 5 kHz. $T_{1/2}$ analysis was performed on serotonin concentration ([serotonin]) vs. time traces using an automated peak finder function with eDAQ Chart software and peak parameters for $t_{1/2}$ analysis (eDAQ, Melbourne, Australia). Students *t*-tests were performed in excel on paired datasets, $p < 0.05$ was taken as statistically significant.

Results

Electrically stimulated *in vivo* serotonin responses

Three different serotonin responses were observed in the mouse SNr after biphasic electrical MFB stimulation (60 Hz, 120 pulses, 350 μA), Fig. 1. Representative color plots are shown in Fig. 1a. Color plots are constructed by displaying

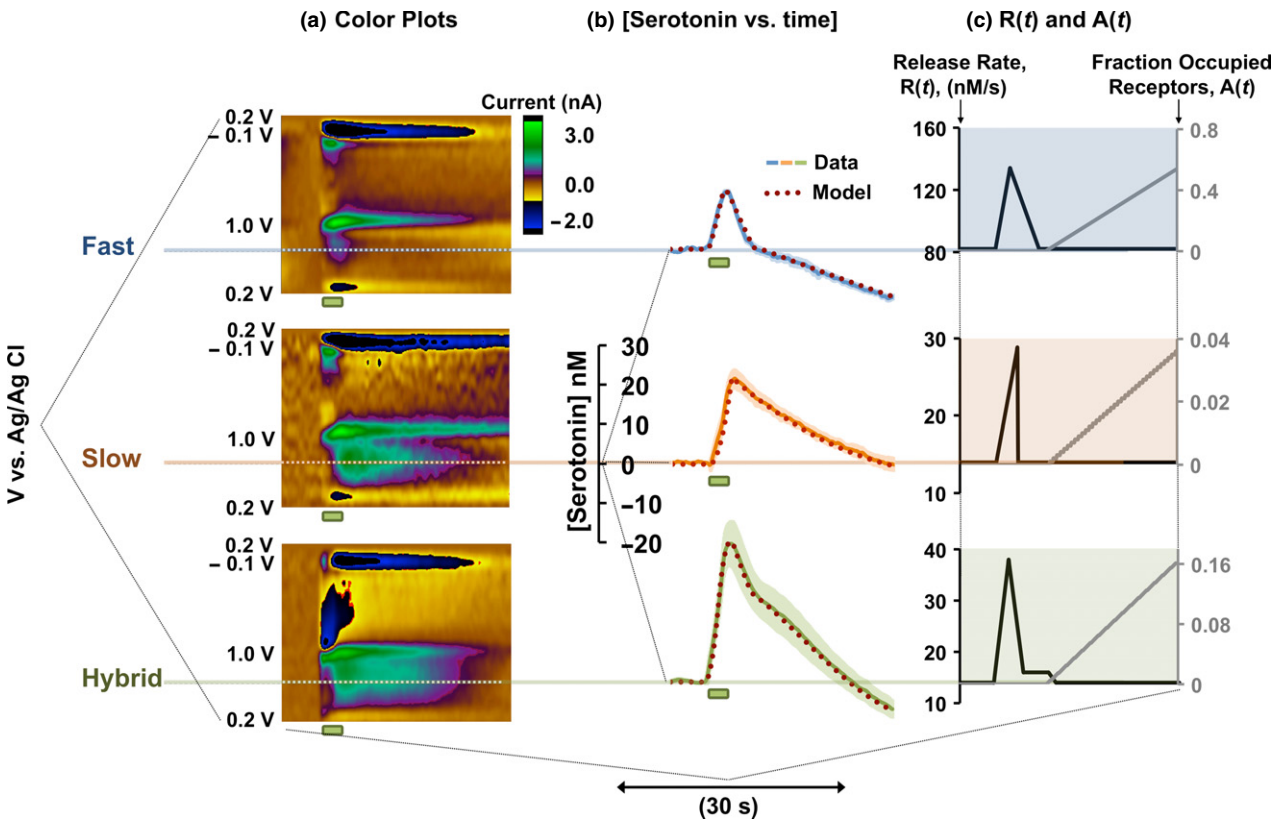

Fig. 1 (a) Representative color plots for fast, slow, and hybrid responses. Stimulation is denoted by green bar under each color plot. (b) Averaged [serotonin] vs. time (solid curves, n = 5 ± SEM) and modeled curve (burgundy dotted) for the three response types. Stimulation is denoted by green bar under each plot. (c) Choices of R(t) and A(t) for fast, slow, and hybrid responses.

substrate identifying cyclic voltammograms (CVs), collected at 10 Hz, with time. The y-axis is potential, the x-axis is time, and the z-axis is a false color scale denoting current. Average [serotonin] versus time plots, taken from the horizontal dashed lines, are shown in Fig. 1b. The green rectangles under the color plots and the [serotonin] versus time plots show the duration of electrical stimulation. We termed these three responses fast (blue solid curve), slow (orange solid curve), and hybrid (green solid curve) based on the shape and slopes of the decay from the peak to the baseline (serotonin clearance). Fast responses decay rapidly ($t_{1/2}$ of clearance < 6 s) with a single slope, slow responses decay sluggishly ($t_{1/2}$ > 6 s) with a single slope and hybrid responses display two slopes, decaying with fast profile for a few seconds, and then switching to slow decay. Average $t_{1/2}$ of the clearance curves of slow responses was 7.8 ± 3.2 s (n = 5 ± SEM), 1.6 ± 0.6 s (n = 5 ± SEM) for fast responses, and 5.9 ± 1.2 s (n = 5 ± SEM) for hybrid responses. Fast responses had significantly lower $t_{1/2}$ than both slow (p < 0.0001) and hybrid (p = 0.007). No statistically significant differences were observed in $t_{1/2}$ between slow and hybrid responses (p = 0.197). The amplitude of fast responses was 13.6 ± 0.7 nM, slow responses 22.9 ± 2.5 nM (n = 5 ± SEM), and hybrid responses 29.6 ± 5.5 nM (n = 5 ± SEM). Fast responses had significantly lower amplitude than both hybrid (p = 0.017) and slow (p = 0.005). No significant difference in amplitude was observed between hybrid and slow responses (p = 0.291). In 67 mice, we found that approximately 20% of responses were fast, 30% were slow, and 50% were hybrid.

To establish that the nature of the three response types is physiological, we tested the kinetic reproducibility of our electrodes in a FIA system. In Fig. 4 we injected serotonin (1 μM) onto eight electrodes. The responses are displayed as an average with SEM. There are negligible differences in electrode kinetics because of the small magnitude of the error bars in the rising portion of the injection.

Modeling *in vivo* voltammetric serotonin responses

Our model, shown below, employs Michaelis–Menten kinetics similar to a model introduced by Wightman and colleagues to describe serotonin kinetics in SNr tissue preparations (Bunin and Wightman 1998). However, our model additionally incorporates two reuptake mechanisms, a basal concentration of serotonin and autoreceptor effects. [$S(t)$] denotes the concentration of serotonin in the SNr extracellular space. We assume that [$S(t)$] satisfies the differential equation:

$$\frac{d[S(t)]}{dt} = R(t)(1 - A(t)) - \alpha\frac{V_{max1}[S(t)]}{K_{m1} + [S(t)]} - \beta\frac{V_{max2}[S(t)]}{K_{m2} + [S(t)]}$$

where R(t) is the rate of release and $A(t)$ is the fraction of stimulated autoreceptors. R(t) does not represent the MFB stimulation but rather neuronal firing in the dorsal raphe nucleus (DRN) and subsequent release of serotonin in the SNr. In our control models (no drugs), firing rises and decays quickly (but not instantaneously) in response to the stimulation because of the non-instantaneous excitation/relaxation of the MFB-DRN-SNr circuitry. V_{max1};K_{m1} and V_{max2};K_{m2} are the V_{max} and K_m values of the two Michaelis–Menten reuptake mechanisms. V_{max1};K_{m1} correspond to slow responses, while V_{max2};K_{m2} correspond to fast responses. The constants α and β are the weights of the two reuptake mechanisms. For fast responses α = 0 and β = 1, for slow responses α = 1 and β = 0. For hybrid responses: α is taken as 1 at all times. We incorporate β in the following way: when [$S(t)$] is > 44 nM, β is 0.03 and then decays linearly to 0 as [$S(t)$] decreases from 44 nM to 39 nM and β = 0 when [$S(t)$] is < 39 nM. This means that the reuptake associated with β is low affinity and therefore loses effectiveness at low concentrations. Thus, hybrid responses have contributions from both reuptake mechanisms.

Figure 1b shows the model curves (burgundy dotted) superimposed onto the three experimental serotonin response types (blue, orange, and green solid curves). We found that the following V_{max} and K_m values fit well to the experimental data: V_{max1};K_{m1} = 17.5 nM s^{-1} and 5 nM and V_{max2};K_{m2} = 780 nM s^{-1} and 170 nM, respectively. The three simulations carried the same V_{max} and K_m values but differed in the choices of α, β, and the R(t) and A(t) functions shown for each response in Fig. 1c. For fast response simulations α = 0, so only the reuptake represented by V_{max2};K_{m2} was present. R(t) rose linearly for 2 s and then decayed linearly over 4 s. A(t) rose linearly after 12 s. For slow response simulations β = 0, such that only the reuptake represented by V_{max1};K_{m1} was present. $R(t)$ rose linearly for 3 s and then returned immediately to baseline. A(t) rose linearly after 12 s with a different slope than the fast responses. For hybrid response simulations both reuptake mechanisms were present. R(t) rose rapidly, fell rapidly, subsequently reaching plateau and returned to baseline. A(t) rose linearly after 12 s, again with a different slope than slow and fast responses.

To model the effects of a hybrid response after SSRI administration, we administered Escitalopram (ESCIT). Figure 2 shows averaged control serotonin responses (black solid curve, n = 5 ± SEM error bars in gray) and averaged responses 120 min after ESCIT administration (100 mg kg^{-1}, shown by teal solid curve, n = 5 ± SEM error bars in light teal). Electrical stimulation duration is denoted by the green bar under the traces. The models are superimposed onto both curves in the burgundy dotted curves. The variation of A(t) and R(t) with time for both curves are inset. The best fit was obtained when Uptake 1 was inhibited by 95% and Uptake 2 by 40%.

Contribution from the serotonin autoreceptors

A common feature of our stimulated serotonin release profiles is that [serotonin] 'dips' below baseline. In Fig. 3a,

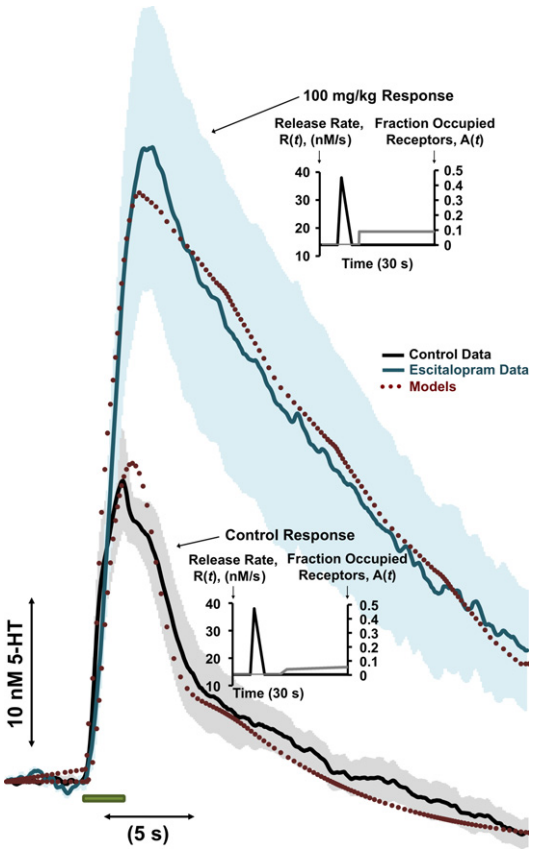

Fig. 2 Averaged [serotonin] versus time trace for a control serotonin response (black curve, n = 5 ± SEM) and 120 min after 100 mg kg^{-1} ESCIT administration (teal curve, n = 5 ± SEM). Stimulation duration is denoted by the green bar under the traces. The models are superimposed onto the traces in the burgundy dashed traces. Choices of A(t) and R(t) are inset for control and ESCIT responses.

a representative serotonin release event is shown. CV_a (inset, taken during the stimulation at point a) represents a typical serotonin CV (with some additional features owing to corelease of histamine obtained in the SNr via MFB stimulation (Hashemi *et al.* 2011a)). CV_b (taken at the point where [serotonin] dips below baseline, b) resembles the concentration inverse of CV_a. When CV_b is reversed and superimposed onto CV_a, there is a good agreement confirming a reduction in [serotonin]. For our model, it was necessary to incorporate an increasing autoreceptor effect (starting 7 s after the beginning of stimulation the function A *(t)* increases linearly) to account for the dip. Both cell body (5-HT1A) and terminal (5-HT1B) autoreceptors that are part of the DRN-MFB-SNr circuit contribute to A*(t)*.

To test our model's suggestion of autoreceptor control experimentally, we treated mice with methiothepin, a non-selective serotonin receptor antagonist, with highest affinity for the serotonin autoreceptors (Monachon *et al.* 1972). Figure 3b (left), shows control (black curve) and the average effects of acute methiothepin (20 mg kg^{-1}) administration ($n = 5 \pm$ SEM) (purple curve). The maximum amplitude was unaffected by this drug: at 24.1 ± 6.7 nM pre-methiothepin and 26.3 ± 5.0 nM 60 min post-methiothepin ($p = 0.489$, $n = 5 \pm$ SEM). The $t_{1/2}$ increased from 3.2 ± 1.1 s to 19.9 ± 5.9 s at 60 min ($p = 0.032$, $n = 5 \pm$ SEM). The control response was treated with the hybrid response model (burgundy dotted curve). We modeled the methiothepin treatment by setting the autoreceptor effect function, A*(t)*, to zero and choosing the release function, R*(t)*, shown in Fig. 3b (right). It is clear, both experimentally and via our model, that methiothepin abolishes serotonin's descent below baseline.

Discussion

Three serotonin response types *in vivo*

Serotonin reuptake is a major focus of antidepressant agents. We previously reported stimulated [serotonin] vs. time in the SNr (Wood and Hashemi 2013) as a composite average of five experiments. Upon accumulation of more datasets, however, it became apparent that responses are heterogeneous, and averaging removes nuances that provide important information about serotonin neurochemistry. We found three distinct serotonin responses to a standard stimulation, primarily differentiated by the clearance slopes. Michael and colleagues found dopamine heterogeneity in the rising portion of extracellular concentration curves and proposed the terminology, slow, fast, and hybrid (Moquin and Michael 2009, 2011), which we adopted here. For serotonin, all three responses have a rapid rise. Fast responses are characterized by a rapid return to baseline, and slow responses are characterized by a more gradual return to baseline. Hybrid responses have both fast and slow attributes because they descend rapidly for a short time and then switch to slow decay.

Differences between electrode kinetics could account for erroneous assignment of our responses. We explore this in Fig. 4. Here, serotonin (1 μM) was injected *in vitro* onto eight electrodes; the responses are shown averaged with SEM. While there are differences in the response amplitude between electrodes, the difference in electrode kinetics is negligible (evidenced by the small error in the initial rising portion of the response shown between the two vertical green dashed lines). Therefore, it is likely that *in vivo* processes underlie our three response types.

Two serotonin reuptake mechanisms

Visual inspection of our three serotonin response types shows two separate clearance slopes, suggesting involvement of two discrete reuptake mechanisms. Simple $t_{1/2}$ analysis did not allow us to distinguish between hybrid and slow responses; therefore, we sought to employ kinetic models to determine any differences. However, we could not model our responses with models established for serotonin release

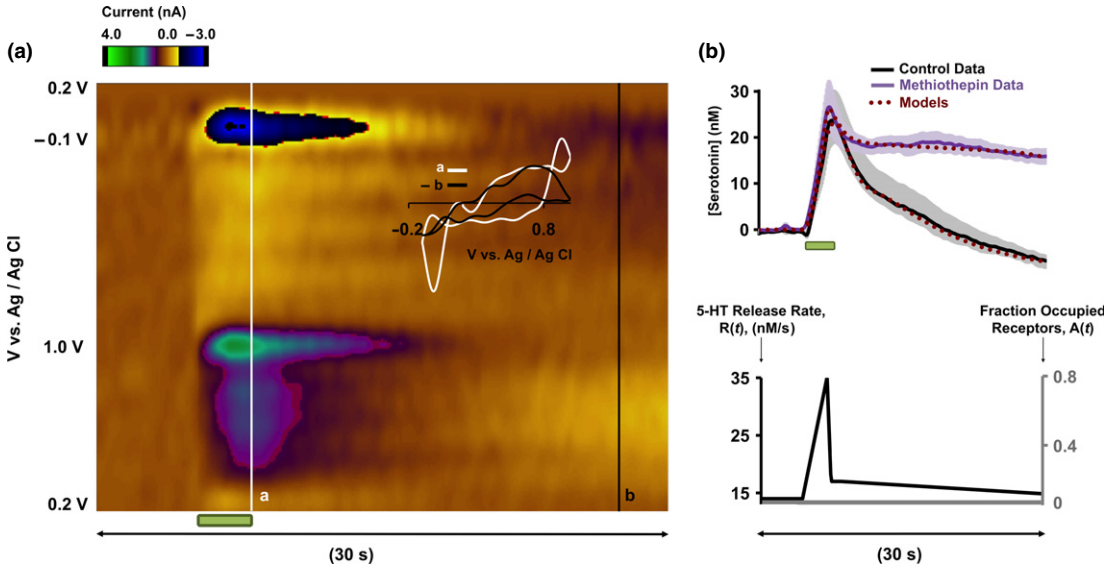

Fig. 3 (a) Representative color plot of a stimulated serotonin event, stimulation duration is denoted by the green bar under the color plot. Inset in (A) – CV_a taken from the vertical white line denoted by a and superimposed onto CV_b which is taken and reversed from the vertical black line denoted by b. (b) (left) – Averaged [serotonin] versus time (solid curves, n = 5 ± SEM) and modeled curves (burgundy dotted) for methiothepin treatment. Stimulation duration is denoted by the green bar under the curves. (b) (right) – A(t) = 0 and the choice of R(t) for the methiothepin simulation.

in tissue slice preparations (Bunin *et al.* 1998). We found that incorporation of two separate reuptake mechanisms into our model, V_{max1};K_{m1} and V_{max2};K_{m2} allowed us to closely model our experimental data. Local stimulations in tissue slice preparations create a massive efflux of serotonin (Bunin and Wightman 1998; Bunin *et al.* 1998). In previous tissue slice experiments, serotonin clearance was apparently dominated by a reuptake mechanism that kinetically mirrors our values for V_{max2};K_{m2} while contributions from V_{max1};K_{m1} were reasonable to neglect. It is interesting that close inspection of [serotonin] versus time traces in these previous experiments (Bunin *et al.* 1998) shows that at low concentrations (low nM) the experimental data deviate from established models. At these low concentrations serotonin begins to decay slowly, in a similar way to our slow responses, described more aptly by V_{max1};K_{m1}.

Snyder and colleagues suggested that serotonin clearance occurred via two reuptake mechanisms (Shaskan and Snyder 1970). They proposed Uptake 1 with high affinity and low efficiency and Uptake 2 with low affinity and high efficiency. Daws and colleagues verified pharmacologically that Uptake 1 is likely to occur primarily via the SERTs on serotonergic neurons and that Uptake 2 includes other transporters on other cells including the dopamine transporter, the norepinephrine transporter (NET), and the organic cation transporter (OCT) (Daws *et al.* 2013; Horton *et al.* 2013). Here, for the first time, we present endogenous *in vivo* data to support the concept of Uptake 1 and Uptake 2. Indeed our values for V_{max1}:K_{m1} (17.5 nM s^{-1} and 5 nM) and V_{max2};

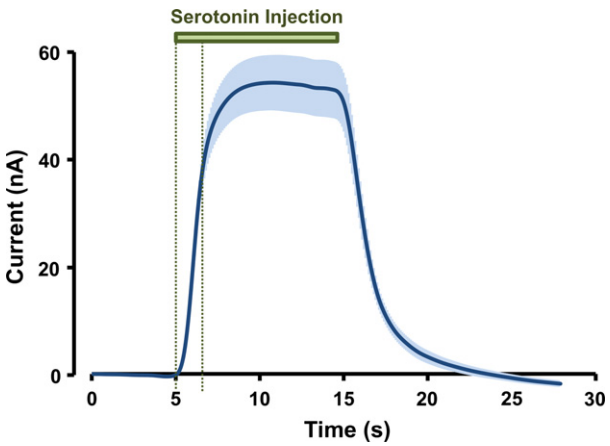

Fig. 4 *In vitro* fast scan cyclic voltammetry (FSCV) response to serotonin (1 μM) in a flow injection analysis (FIA) cell ($n = 8$ electrodes ± SEM). The green bar indicates the duration of serotonin injection. The two vertical green dashed lines indicate the rising response portion of the signal.

K_{m2} (780 nM s^{-1} and 170 nM) agree remarkably well with high affinity, low efficiency uptake (Uptake 1), and with low affinity, high efficiency uptake (Uptake 2) respectively.

In vivo serotonin release is known to be highly regulated, and $[serotonin]_{evoked}$ is in the low nM range (Hashemi *et al.* 2009, 2011a, 2012; Wood and Hashemi 2013). Furthermore, it has been demonstrated that inhibiting serotonin reuptake and metabolism (with an SSRI and MAOI) leads to the

potentially fatal serotonin syndrome (Hashemi *et al.* 2012). Therefore, it is not remarkable for multiple reuptake mechanisms to be charged with clearing serotonin from the synapse. It is probable that physiologically released serotonin is at low enough concentrations such that low efficiency, high affinity SERTs on serotonergic neurons, Uptake 1, can reuptake serotonin effectively. However, if serotonin release exceeds a certain limit, it may diffuse to other transport mechanisms, which are not as selective for serotonin and therefore have low affinity, but operate at high efficiency (Uptake 2).

To probe the effects of a commonly prescribed SSRI mechanistically, we administered ESCIT at a high dose. We chose to administer 100 $mgkg^{-1}$ and compare data taken at 120 min after drug administration based on previous dose–response experiments that showed maximal and lingering effects with this dose and at this time (Wood and Hashemi 2013). Figure 2 shows the experimental data and corresponding models. SSRI administration substantially increased serotonin release and decreased its clearance, as previously seen (Wood and Hashemi 2013). This is not surprising since ESCIT is highly selective for the SERTs (Uptake 1). However, after considerable experimentation we found that our data were best fit with a model that included 95% inhibition of Uptake 1 and 40% inhibition of Uptake 2. This is not surprising given that there is evidence that SSRIs have affinity for Uptake 2 transporters. For example, ESCIT has been found to block NETs and have a significant effect upon OCT-sensitive serotonin uptake (Nguyen *et al.* 2013). Furthermore, many SSRIs inhibit the human plasma membrane monoamine transporter, also an Uptake 2 transporter (Haenisch and Bonisch 2010). Finally, Horton *et al.* (2013) found that, in the presence of fluvoxamine, blockage of Uptake 2 by Decynium-22 greatly raised both the extracellular 5-HT level and the clearance time.

It is important to note that the high dose of ESCIT in our experiment (100 $mgkg^{-1}$) exceeds the minimal effective dose required for behavioral effects in mice (12 $mgkg^{-1}$) (Sanchez *et al.* 2003). Although not likely to be encountered clinically, the high dose enables us to illustrate a central point in this work: that physiological deviations above normal extracellular serotonin concentration are cleared via SERTs, but larger deviations are cleared through combination of the SERTs and Uptake 2 transporters. Since different SSRIs have different chemical compositions, it is reasonable to expect that, at a given concentration, each blocks some percentage of Uptake 1 and a (presumably lower) percentage of Uptake 2. Thus, one would expect that both peak response and clearance time would vary among different SSRIs.

Serotonin autoreceptor regulation of serotonin transmission

FSCV does not determine the baseline or steady-state value of the extracellular serotonin concentration; this is an essential, previously unaccounted for, component of kinetic models for serotonin. The experimental curve for fast response (Fig. 1) descends 10–20 nM below baseline. While we cannot know what the absolute levels are, our data imply that the steady-state concentration of serotonin is between 10 and 20 nM; we therefore assumed $[serotonin]_{baseline}$ in our simulations as 20 nM. After completing simulations, we subtracted 20 nM from the model curves so that we could compare them directly to the experimental curves that are plotted with baseline as 0 nM. The value of 20 nM is not surprising because previous estimations of basal neurotransmitter concentrations (Justice 1993) are now thought to have underestimated the true concentrations (Wang *et al.* 2010; Owesson-White *et al.* 2012). In Fig. 1, and in most of our experimental data, [serotonin] dips below this baseline after stimulation has ceased. While a dip below baseline has previously been attributed to pH shifts for dopamine experiments (Venton *et al.* 2003), comparison of cyclic voltammograms suggests that this dip is, indeed, a substantial reduction in extracellular serotonin.

It was, again, not possible to utilize traditional models to account for this dip, likely because of the inherent differences between serotonin regulation in tissue slice preparations and *in vivo*. Autoreceptors are known to inhibit serotonin release (Barnes and Sharp 1999), in particular, prior FSCV studies in tissue slice preparations and chronoamperometry studies in synaptosomes and *in vivo* have uncovered important, discrete roles for different autoreceptor subtypes (Daws *et al.* 1999, 2000; Hopwood and Stamford 2001; Roberts and Price 2001; Threlfell *et al.* 2010; Hagan *et al.* 2012). In tissue slice experiments autoreceptors likely function differently than in *in vivo* because the cell body-terminal connections are severed. *In vivo,* in our circuitry, serotonin released from the DRN cell bodies stimulates 5-HT1A autoreceptors and serotonin released in SNr acts on 5-HT1B autoreceptors (Barnes and Sharp 1999). Therefore, we postulated that our dip below baseline could be autoreceptor mediated. Indeed, the gradually increasing autoreceptor effect in the model captures the experimental data very well. This is novel chemical data that implies ambient autoreceptor effects and the time scale on which they operate.

To experimentally test this autoreceptor hypothesis we employed methiothepin, a non-selective serotonin receptor antagonist with most affinity for the serotonin autoreceptors, to target the multiple autoreceptors that are involved in the DRN-SNr circuitry (Barnes and Sharp 1999). A prior FSCV study in DRN slices showed that combined 5-HT1A and 5-HT1B receptor antagonism produced greater serotonin efflux than targeting either receptor alone (Roberts and Price 2001). In our study, methiothepin greatly increased the $t_{1/2}$ of clearance of our experimental data and our model could fit the experimental data by removing $A(t)$. This simple, yet effective modeling strategy gives further evidence that autoreceptors may be acting within the timeframe of our collection window (30 s) to reduce serotonin transmission.

The advantage of our model is its simplicity; however, it carries limitations. The product term, R*(t)*(1-A(*t*)), cannot distinguish between lowering R(*t*) and raising A(*t*). For example, the autoreceptor effect may proceed earlier than 7 s after initiation of the stimulation. Here, we considered R(*t*) as release in the absence of autoreceptors and (1 – A(*t*)) as the modification of release when the autoreceptors are stimulated. We assumed that R(*t*) rapidly increased and decreased in correspondence to the stimulus and A(*t*) increased gradually thereafter (Fig. 1c). An additional limitation is that we cannot yet distinguish between the different serotonin autoreceptors. Finally, our data imply that basal serotonin levels are around 20 nM; this level needs to be verified independently with a method capable of reporting basal serotonin levels at carbon fiber microelectrodes. Addressing these three limitations requires method development, elaborate pharmacological experiments, a more sophisticated modeling approach (Reed *et al.* 2012) and is the focus of our future work.

We studied endogenous serotonin release and reuptake with FSCV. We took a novel mathematical approach by treating the data with Michaelis–Menten kinetics that incorporated two reuptake mechanisms, a baseline serotonin concentration, and autoreceptor functions. Experimentally, we discovered three serotonin chemical signatures which we termed fast, slow, and hybrid and mathematically we found that they could be explained with two reuptake mechanisms. We found a high affinity, low efficiency reuptake mechanism (Uptake 1), proposed to be via the SERTs and a low affinity, high efficiency reuptake system (Uptake 2) thought to represent the contribution of dopamine transporters, NETs, and OCTs. In addition, we outlined a timeframe for the inhibitory role of autoreceptors. Combining voltammetric and theoretical approaches gives us an ideal tool to study serotonin's dual-uptake mechanisms and autoreceptor control. This capability will be invaluable for characterizing the mechanisms of the pharmacological effects of existing antidepressant agents and to aide in the design of novel agents.

Acknowledgements and conflict of interests disclosure

WSU start-up funds (PH), NSF grants EF-1038593 (HFN,MR), NSF agreement 0112050 through the Mathematical Biosciences Institute (JB, MR), an NSF CAREER Award (JB), the Alfred P. Sloan Foundation (JB) and NIH grant R01 ES019876 (DT) supported this research.

All experiments were conducted in compliance with the ARRIVE guidelines. The authors have no conflict of interest to declare.

References

Alexander G. C., Gallagher S. A., Mascola A., Moloney R. M. and Stafford R. S. (2011) Increasing off-label use of antipsychotic medications in the United States, 1995-2008. *Pharmacoepidemiol. Drug Saf.* **20**, 177–184.

Barnes N. M. and Sharp T. (1999) A review of central 5-HT receptors and their function. *Neuropharmacology* **38**, 1083–1152.

Blier P., de Montigny C. and Chaput Y. (1987) Modifications of the serotonin system by antidepressant treatments: implications for the therapeutic response in major depression. *J. Clin. Psychopharmacol.* **7**, 24S–35S.

Bunin M. A. and Wightman R. M. (1998) Quantitative evaluation of 5-hydroxytryptamine (serotonin) neuronal release and uptake: an investigation of extrasynaptic transmission. *J. Neurosci.* **18**, 4854–4860.

Bunin M. A., Prioleau C., Mailman R. B. and Wightman R. M. (1998) Release and uptake rates of 5-hydroxytryptamine in the dorsal raphe and substantia nigra reticulata of the rat brain. *J. Neurochem.* **70**, 1077–1087.

Chaput Y., de Montigny C. and Blier P. (1986) Effects of a selective 5-HT reuptake blocker, citalopram, on the sensitivity of 5-HT autoreceptors: electrophysiological studies in the rat brain. *Naunyn-Schmiedeberg's Arch. Pharmacol.* **333**, 342–348.

Cipriani A., Furukawa T. A., Salanti G. *et al.* (2009) Comparative efficacy and acceptability of 12 new-generation antidepressants: a multiple-treatments meta-analysis. *Lancet* **373**, 746–758.

Davies M. A., Sheffler D. J. and Roth B. L. (2004) Aripiprazole: a novel atypical antipsychotic drug with a uniquely robust pharmacology. *CNS Drug Rev.* **10**, 317–336.

Daws L. C., Gerhardt G. A. and Frazer A. (1999) 5-HT1B antagonists modulate clearance of extracellular serotonin in rat hippocampus. *Neurosci. Lett.* **266**, 165–168.

Daws L. C., Gould G. G., Teicher S. D., Gerhardt G. A. and Frazer A. (2000) 5-HT(1B) receptor-mediated regulation of serotonin clearance in rat hippocampus in vivo. *J. Neurochem.* **75**, 2113–2122.

Daws L. C., Koek W. and Mitchell N. C. (2013) Revisiting serotonin reuptake inhibitors and the therapeutic potential of "uptake-2" in psychiatric disorders. *ACS Chem. Neurosci.* **4**, 16–21.

Ferguson J. M. (2001) SSRI Antidepressant Medications: Adverse Effects and Tolerability. *Prim. Care Companion J. Clin. Psychiatry* **3**, 22–27.

Gelenberg A. J. and Chesen C. L. (2000) How fast are antidepressants? *J. Clin. Psychiatry* **61**, 712–721.

Gonzalez O., Berry J. T., Mcknight-Eily L. R., Strine T., Edwards K. W. and Croft J. B. (2010) Current depression among adults - United States, 2006 and 2008, in *Morbidity and Mortality Weekly Report* (Moolenaar R.L., ed.), pp. 1229–1258. Center for Disease Control and Prevention, Hyattsvilles.

Haenisch B. and Bonisch H. (2010) Interaction of the human plasma membrane monoamine transporter (hPMAT) with antidepressants and antipsychotics. *Naunyn Schmiedebergs Arch. Pharmacol.* **381**, 33–39.

Hagan C. E., McDevitt R. A., Liu Y., Furay A. R. and Neumaier J. F. (2012) 5-HT(1B) autoreceptor regulation of serotonin transporter activity in synaptosomes. *Synapse* **66**, 1024–1034.

Hashemi P., Dankoski E. C., Petrovic J., Keithley R. B. and Wightman R. M. (2009) Voltammetric Detection of 5-Hydroxytryptamine Release in the Rat Brain. *Anal. Chem.* **81**, 9462–9471.

Hashemi P., Dankoski E. C., Wood K. M., Ambrose R. E. and Wightman R. M. (2011a) In vivo electrochemical evidence for simultaneous 5-HT and histamine release in the rat substantia nigra pars reticulata following medial forebrain bundle stimulation. *J. Neurochem.* **118**, 749–759.

Hashemi P., Walsh P. L., Guillot T. S., Gras-Najjar J., Takmakov P., Crews F. T. and Wightman R. M. (2011b) Chronically Implanted, Nafion-Coated Ag/AgCl Reference Electrodes for Neurochemical Applications. *ACS Chem. Neurosci.* **2**, 658–666.

Hashemi P., Dankoski E. C., Lama R., Wood K. M., Takmakov P. and Wightman R. M. (2012) Brain dopamine and serotonin differ in regulation and its consequences. *Proc. Natl Acad. Sci. USA* **109**, 11510–11515.

Hopwood S. E. and Stamford J. A. (2001) Multiple 5-HT(1) autoreceptor subtypes govern serotonin release in dorsal and median raphe nuclei. *Neuropharmacology* **40**, 508–519.

Horton R. E., Apple D. M., Owens W. A. *et al.* (2013) Decynium-22 enhances SSRI-induced antidepressant-like effects in mice: uncovering novel targets to treat depression. *J. Neurosci.* **33**, 10534–10543.

Jackson B. P., Dietz S. M. and Wightman R. M. (1995) Fast-scan cyclic voltammetry of 5-hydroxytryptamine. *Anal. Chem.* **67**, 1115–1120.

Justice J. B., Jr (1993) Quantitative microdialysis of neurotransmitters. *J. Neurosci. Methods* **48**, 263–276.

Le Poul E., Laaris N., Doucet E., Laporte A. M., Hamon M. and Lanfumey L. (1995) Early desensitization of somato-dendritic 5-HT1A autoreceptors in rats treated with fluoxetine or paroxetine. *Naunyn-Schmiedeberg's Arch. Pharmacol.* **352**, 141–148.

Masand P. S. and Gupta S. (2002) Long-term side effects of newer-generation antidepressants: SSRIS, venlafaxine, nefazodone, bupropion, and mirtazapine. *Ann. Clin. Psychiatry* **14**, 175–182.

Monachon M. A., Burkard W. P., Jalfre M. and Haefely W. (1972) Blockade of central 5-hydroxytryptamine receptors by methiothepin. *Naunyn Schmiedebergs Arch. Pharmacol.* **274**, 192–197.

Moquin K. F. and Michael A. C. (2009) Tonic autoinhibition contributes to the heterogeneity of evoked dopamine release in the rat striatum. *J. Neurochem.* **110**, 1491–1501.

Moquin K. F. and Michael A. C. (2011) An inverse correlation between the apparent rate of dopamine clearance and tonic autoinhibition in subdomains of the rat striatum: a possible role of transporter-mediated dopamine efflux. *J. Neurochem.* **117**, 133–142.

Nguyen H. T., Guiard B. P., Bacq A., David D. J., David I., Quesseveur G., Gautron S., Sanchez C. and Gardier A. M. (2013) Blockade of the high-affinity noradrenaline transporter (NET) by the selective 5-HT reuptake inhibitor escitalopram: an in vivo microdialysis study in mice. *Br. J. Pharmacol.* **168**, 103–116.

Owesson-White C. A., Roitman M. F., Sombers L. A., Belle A. M., Keithley R. B., Peele J. L., Carelli R. M. and Wightman R. M. (2012) Sources contributing to the average extracellular concentration of dopamine in the nucleus accumbens. *J. Neurochem.* **121**, 252–262.

Paxinos G. and Franklin K. B. (2008) *The Mouse Brainiin Stereotaxic Coordinates*. Academic Press, Waltham, MA.

Reed M. C., Nijhout H. F. and Best J. A. (2012) Mathematical insights into the effects of levodopa. *Front. Integr. Neurosci.* **6**, 21.

Riad M., Zimmer L., Rbah L., Watkins K. C., Hamon M. and Descarries L. (2004) Acute treatment with the antidepressant fluoxetine internalizes 5-HT1A autoreceptors and reduces the in vivo binding of the PET radioligand [18F]MPPF in the nucleus raphe dorsalis of rat. *J. Neurosci.* **24**, 5420–5426.

Richelson E. and Souder T. (2000) Binding of antipsychotic drugs to human brain receptors focus on newer generation compounds. *Life Sci.* **68**, 29–39.

Roberts C. and Price G. W. (2001) Interaction of serotonin autoreceptor antagonists in the rat dorsal raphe nucleus: an in vitro fast cyclic voltammetry study. *Neurosci. Lett.* **300**, 45–48.

Sanchez C., Bergqvist P. B., Brennum L. T., Gupta S., Hogg S., Larsen A. and Wiborg O. (2003) Escitalopram, the S-(+)-enantiomer of citalopram, is a selective serotonin reuptake inhibitor with potent effects in animal models predictive of antidepressant and anxiolytic activities. *Psychopharmacology* **167**, 353–362.

Shaskan E. G. and Snyder S. H. (1970) Kinetics of serotonin accumulation into slices from rat brain: relationship to catecholamine uptake. *J. Pharmacol. Exp. Ther.* **175**, 404–418.

Souery D., Papakostas G. I. and Trivedi M. H. (2006) Treatment-resistant depression. *J. Clin. Psychiatry* **67**(Suppl 6), 16–22.

Spielmans G. I., Berman M. I., Linardatos E., Rosenlicht N. Z., Perry A. and Tsai A. C. (2013) Adjunctive atypical antipsychotic treatment for major depressive disorder: a meta-analysis of depression, quality of life, and safety outcomes. *PLoS Med.* **10**, e1001403.

Threlfell S., Greenfield S. A. and Cragg S. J. (2010) 5-HT(1B) receptor regulation of serotonin (5-HT) release by endogenous 5-HT in the substantia nigra. *Neuroscience* **165**, 212–220.

Venton B. J., Michael D. J. and Wightman R. M. (2003) Correlation of local changes in extracellular oxygen and pH that accompany dopaminergic terminal activity in the rat caudate-putamen. *J. Neurochem.* **84**, 373–381.

Wang Y., Moquin K. F. and Michael A. C. (2010) Evidence for coupling between steady-state and dynamic extracellular dopamine concentrations in the rat striatum. *J. Neurochem.* **114**, 150–159.

Wood K. M. and Hashemi P. (2013) Fast-scan cyclic voltammetry analysis of dynamic serotonin reponses to acute escitalopram. *ACS Chem. Neurosci.* **4**, 715–720.

Yatham L. N., Goldstein J. M., Vieta E., Bowden C. L., Grunze H., Post R. M., Suppes T. and Calabrese J. R. (2005) Atypical antipsychotics in bipolar depression: potential mechanisms of action. *J. Clin. Psychiatry* **66**(Suppl 5), 40–48.

